



ELSEVIER

Catalysis Today 52 (1999) 197–221



www.elsevier.com/locate/cattod

Fixed bed reactors

P. Andrigo^{*}, R. Bagatin, G. Pagani

EniChem, Corporate Research Centre, Via Fauser 4, 28100 Novara, Italy

Abstract

The present paper presents the phenomena occurring in fixed bed reactors spanning, from the small scale of single pellet, where reaction and diffusion are competing, to the macroscale of whole apparatus, where dispersion and heat transfer play an important role; the most important models used in describing the behaviour of fixed bed reactors and the dependence of most relevant parameters from the geometrical characteristics of the reactor and from the physical properties of the reacting gases are examined. Advice is given in order to design the reactor choosing the governing parameters in order to have stable and effective performance, avoiding situations with multiple solutions and hence potential instability problems. © 1999 Elsevier Science B.V. All rights reserved.

Keywords: Fixed bed reactors; Catalytic reactors; Catalytic pellet; Heat and mass transfer; Heat and mass dispersion; Models

1. Introduction

Packed beds of catalyst particles is the most widely used reactor type for gas phase reactants in the production of large scale basic chemicals and intermediates. In Table 1 some examples of industrial processes are presented.

Fixed bed reactors have also been increasingly used in recent years to treat harmful and toxic substances: the removal of nitrogen oxides from power station flue gases and automobile exhaust purification represent by far the most widely employed applications.

Several reactor configurations are encountered in practice, but it is convenient to differentiate between reactors for adiabatic operation and for nonadiabatic operation.

The analysis of these reactors spans from the micro-scale, with the pellet and its pore structure where the phenomena of reaction and diffusion occur, to the macroscale, with its geometry and the characteristics of reactor bed where the phenomena of heat and mass convection, dispersion and transfer occur.

2. The catalytic pellet

The performance of a shaped catalyst (tablet, extruded, sphere) depends on various factors such as the chemical composition of the active components, promoters and inhibitors, the supported crystallite size and structure distribution, and the synergistic influence of the support. The influence of transport processes on the activity and selectivity of single pellets is the most valuable information in development of new catalysts and is a prerequisite for the rational design and control of a catalytic reactor.

^{*}Corresponding author. Tel.: +39-321-447510;

fax: +39-321-447233

E-mail address: pietro_andrigo@hq.enichem.geis.com (P. Andrigo)

Table 1
Some industrial catalytic reactions

Reaction	Raw material	Product
Hydrogenation/dehydrogenation	Benzene	Cyclohexane
	Acetone	Isopropyl alcohol
	Nitrobenzene	Aniline
	Phenol	Cyclohexanol, cyclohexanon
	Ethylbenzene	Styrene
Oxidation	<i>o</i> -Xylene, naphthalene	Phthalic anhydride
	Ethylene	Ethylene oxide, acetaldehyde
	Methanol	Formaldehyde
	Butylene	Maleic anhydride
	Ethanol	Acetic acid
Addition	Acetylene, HCl	Vinyl chloride
	Acetylene, acetic acid	Vinyl acetate
Others	Propylene, NH ₃ , O ₂	Acrylonitrile
	N ₂ , H ₂	Ammonia

2.1. The diffusion coefficients

The geometrical structure of a catalytic porous pellet consists of a large number of interconnected pores with irregular shapes on which active catalytic components, e.g. noble metals, zeolites, etc. are dispersed; in certain cases, e.g. with mixed oxides, there is a bulk activity generated by main components. Inside the pores three different mechanisms may cause isothermal transport of nonadsorbed gaseous species: the Knudsen diffusion, when the diameters of the pores is much smaller than the mean free path of the gas; the gaseous bulk diffusion when the diameter of the pores is much larger than the mean free path of the gaseous molecules; viscous or bulk flow due to the presence of a pressure gradient.

The pellet may be represented by a single phase continuous (pseudo-homogeneous) model adequate for qualitative and quantitative prediction of most properties of engineering relevance. Inside the pellet the transport of single component j of the gaseous mixture is described by the effective diffusion coefficient D_{esj} , which is in general a function of composition and can be considered constant in simple cases.

A simple model of diffusion for two species ($j=1,2$) is presented by Johnson and Stewart [1]:

$$D_{es1} = \frac{\epsilon_s}{\tau_s} \int_0^\infty \left(\frac{1 - (1 - \sqrt{M_1/M_2}) \cdot y_1}{D_{12}} + \frac{1}{D_{K1}} \right)^{-1} \cdot f(r) dr, \quad (1)$$

where D_{12} is the binary diffusion coefficient (order of magnitude 10^{-4} – 10^{-6} m²/s), D_{K1} the Knudsen coefficient for A_1 (order of magnitude 10^{-6} – 10^{-10} m²/s), ϵ_s the internal porosity of the pellet measurable by well-known porosimetric techniques, τ_s the pellet tortuosity, index of mechanical complexity of the pore structure, $f(r) dr$ is the fraction of the void volume occupied by pores with radii between r and $r+dr$.

Examples of the pore distribution of industrial catalysts are given in Fig. 1 (monodispersed, lower drawing and bidispersed, upper drawing).

For an isotropic pellet $\epsilon_s/\tau_s=1/3$, but in general ϵ_s/τ_s lies in the range $1/3$ – $1/10$ and has to be determined experimentally. Aris [2] and Luss [3] give references for the experimental measurement of the effective diffusivity.

For diffusion inside zeolites (usually supported or included crystallites) we do not have at the moment

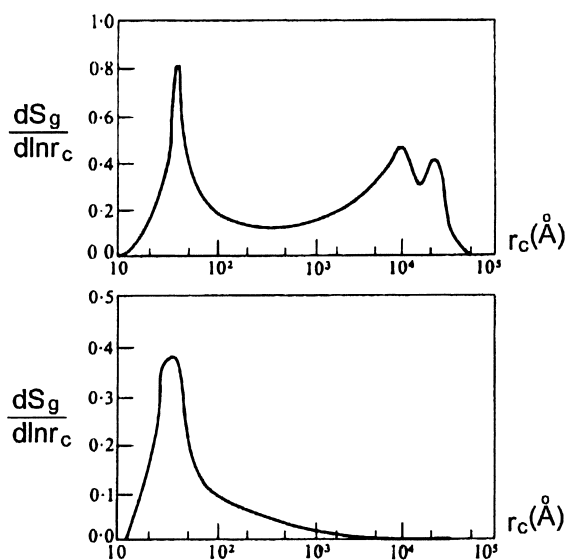


Fig. 1. The distribution of pore size in two typical catalysts: (a) monodisperse (lower curve), (b) bidisperse ($r_c = d_{\text{pore}}/2$; S_g = specific area of catalyst). After Aris [2]; by permission from Oxford University Press.

any a priori correlation; only a broad range (10^{-8} – 10^{-15} m^2/s) and many measurement techniques, most of them based on frequency response analysis as presented by Rees [4].

2.2. The single pellet model

The impact on the reaction of the consecutive diffusion processes of reagents and products from the bulk phase to the active centres and vice versa is expressed by the effectiveness factor, η , equal to the ratio between the observed rate and the hypothetical rate if the composition and temperature throughout the pellet would be uniform and equal to that of the pellet surface (or to that of the surrounding fluid). Considering a system of NS chemical species and NR reactions $\sum_{j=1}^{\text{NS}} \nu_{ij} \cdot A_j = 0$; $i=1,2,\dots,\text{NR}$, the differential equations for the mass balance of every reactant (product) A_j and the energy balance inside a spherical pellet are:

$$\frac{1}{r^2} \cdot \frac{d}{dr} \left(D_{esj}(\underline{C}_s) \cdot r^2 \cdot \frac{dC_{sj}(r)}{dr} \right) + \rho_s \cdot \mathfrak{R}_j(\underline{C}_s, T_s) = 0, \quad (2)$$

$$\frac{\lambda_{es}}{r^2} \cdot \frac{d}{dr} \left(r^2 \cdot \frac{dT_s(r)}{dr} \right) + \rho_s \cdot \sum (-\Delta H_i) \cdot r_i(\underline{C}_s, T_s) = 0, \quad (3)$$

where \mathfrak{R}_j is the rate of production of species j , $\mathfrak{R}_j = \sum_{i=1}^{\text{NR}} \nu_{ij} \cdot r_i$; and $r_i(\underline{C}_s, T_s)$ is the rate of i th reaction.

In the following boundary conditions [b.c.] (a) points out the absence and (b) the presence of heat and mass transfer limitations: at $r=0$,

$$\frac{dC_{sj}}{dr} = \frac{dT_s}{dr} = 0, \quad (4)$$

at $r=(d_p/2)$,

$$C_{sj} = C_{ssj} \quad (5a)$$

or

$$\epsilon_s \cdot k_{gj} \cdot (C_{ssj} - C_j) = -D_{esj} \cdot \frac{dC_{sj}}{dr} \Big|_{r=d_p/2}, \quad (5b)$$

$$T_s = T_{ss} \quad (6a)$$

or

$$h_g \cdot (T_{ss} - T) = \lambda_{es} \cdot \frac{dT_s}{dr} \Big|_{r=d_p/2}, \quad (6b)$$

where the mass transfer (k_{gj}) and heat transfer (h_g) coefficients are the bridge between surface conditions (C_{ssj} and T_{ss}) and bulk gas conditions (C_j and T).

Fig. 2 gives a picture of concentration and temperature profiles which develop inside the pellet and

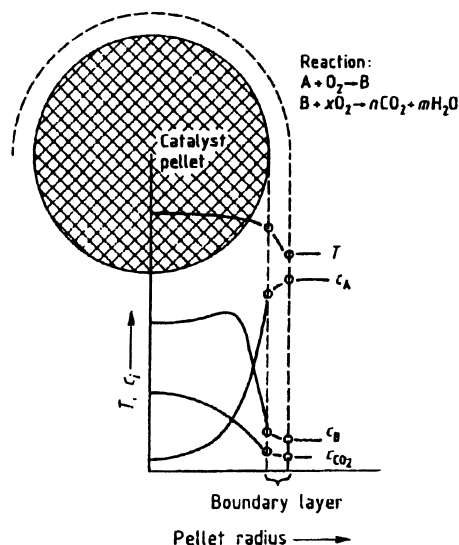


Fig. 2. Temperature and concentration profiles for a partial oxidation reaction in a spherical catalyst pellet.

across the boundary layer, with reference to a possible case.

The equations presented before are rigorous for reactions without volume change and can be considered valid for diluted systems.

Modern methods for the rigorous numerical integration of equations are now feasible tools; e.g. orthogonal spline collocation proposed by Villadsen and Michelsen [5] permit in many cases – with not too much high gradients – rapid and accurate calculations.

2.2.1. Heat transfer parameters

The values of mass transfer coefficients k_{gj} and h_g and of the related dimensionless parameters Sherwood number $Sh_j = k_{gj} \cdot d_p / D_{jm}$ and Nusselt number $Nu = h_g \cdot d_p / \lambda_f$ can be computed by relationships involving the concept of j -factor both for mass (j_{D_j}) and heat (j_H):

$$j_{D_j} = \frac{k_{gj} \cdot \bar{M}}{G} \cdot Sc_j^{2/3} = \frac{a_1}{Re^{b_1}}, \quad (7)$$

$$j_H = \frac{h_g}{G \cdot c_{pf}} \cdot Pr^{2/3} = \frac{a_2}{Re^{b_2}}, \quad (8)$$

where G is the specific mass flow of the reactor inside which our pellet is considered and a_1 , b_1 , a_2 , b_2 are constants; Sc_j (Schmidt number) $= \mu_f / \rho_f D_{jm}$, Pr (Prandtl number) $= c_{pf} \mu_f / \lambda_f$. Consolidated parameters and examples can be found in [6,7].

2.3. The isothermal pellet

Considering an isothermal spherical pellet where a first order reaction $A_1 \rightarrow \text{products}$ is running ($-\rho_s \cdot \Re(C_s, T_s) = k' \cdot \rho_s \cdot C_s = k \cdot C_s$), with the introduction of the dimensionless variables $r^* = r / (d_p/2)$ and $C_s^* = C_s / C_{ss}$ the solution of Eq. (1) is and the effectiveness factor η are given by:

$$C_s^*(r^*) = \frac{\sinh(\phi_r \cdot r^*)}{r^* \cdot \sinh(\phi_r)}, \quad (9)$$

$$\eta = \frac{4\pi \cdot (d_p/2)^2 \cdot D_{es} \cdot (dC_s/dr)|_{(d_p/2)}}{4/3\pi \cdot (d_p/2)^3 \cdot k \cdot C_{ss}} = \frac{3}{\phi_r^2} \cdot (\phi_r \cdot \coth \phi_r - 1), \quad (10)$$

where $\phi_r = (d_p/2) \cdot \sqrt{k/D_{es}}$ is the Thiele modulus (in spherical coordinates).

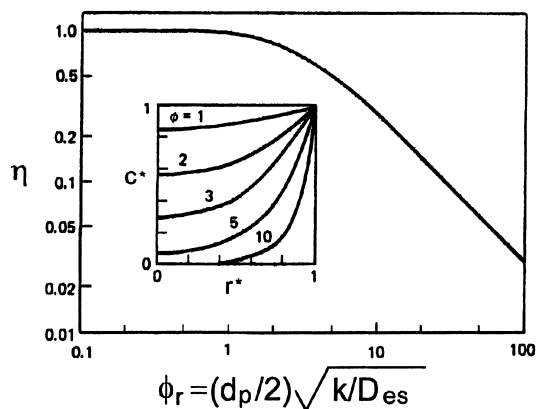


Fig. 3. The effectiveness factor η vs. the Thiele modulus ϕ_r for a first order reaction in a spherical pellet. After Luss [3], by permission from Prentice-Hall.

For small ϕ_r the effectiveness factor is close to unity, indicating that the diffusion resistance has a negligible influence on the observed reaction rate; for large ϕ_r , the effectiveness factor approaches the asymptote $3/\phi_r$, and the diffusion resistance causes a significant reduction of the reaction rate as illustrated in Fig. 3.

When the external mass transfer resistance is not negligible, the concentration and the effectiveness factor for a spherical pellet with reference to the bulk conditions are given by:

$$C_s^*(r^*) = \frac{\sinh(\phi_r \cdot r^*)}{r^* \cdot [\sinh \phi_r + \frac{1}{Sh^*} (\phi_r \cdot \cosh \phi_r - \sinh \phi_r)]}, \quad (11)$$

$$\frac{1}{\eta_b} = \frac{1}{\eta} + \frac{\phi^2}{3Sh^*}, \quad (12)$$

where $Sh^* = \epsilon_s \cdot k_g \cdot (d_p/2) / D_{es}$ (modified Sh number).

For pellets of different shape (sphere, infinite cylinder and infinite slab) the asymptotic value of η for high values of Thiele modulus is different. Using a normalised Thiele modulus $\phi = V_p / S_p \cdot \sqrt{k/D_{es}}$, the asymptotes are brought together (Fig. 4).

In most practical cases Sh^* is at least of order 10; it follows from Eq. (12) that in such a case external mass transfer limitations affect η_b only for large values of ϕ for which important internal diffusion resistance exists.

For a single reaction in an isothermal pellet a

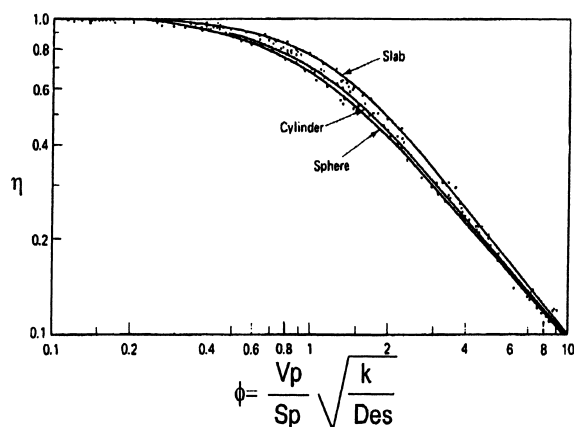


Fig. 4. Effectiveness factor η vs. normalized Thiele modulus ϕ for a first order reaction. Reprinted from Aris and Rester [32]; © 1969 with permission from Pergamon Press.

normalised Thiele modulus is given by

$$\phi = \frac{V_p \cdot r(C_{ss})}{S_p} \cdot \frac{1}{\left(2 \int_{C_{seq}}^{C_{ss}} D_{es}(C_s) \cdot r(C_s) dC_s\right)^{1/2}}, \quad (13)$$

where C_{seq} is zero or the concentration at chemical equilibrium and the effectiveness factor η can be found using the graph of Fig. 4 for a rapid estimate before using more precise methods.

2.3.1. Masking of the intrinsic form of kinetics of rate expression

Diffusion limitations cause several difficulties in the interpretation of kinetic data.

As an example consider an n th order irreversible reaction $A_1 \rightarrow \text{products}$ for which the reaction rate per unit volume of catalyst and the Thiele modulus are $r = A \exp(-E/RT) \cdot C_s^n \cdot \eta$ and $\phi = V_p/S_p \cdot \sqrt{k \cdot C_{ss}^{n-1}/D_{es}}$. For small values of ϕ , η is very close to unity with apparent reaction order $n' = n$ and apparent activation energy $E' = E$. However, when ϕ is large n' tends to $(n+1)/2$ and E' tends to $1/2E$ (see [3] for the simple mathematical steps).

This means heavy limitations for intrinsic order of reaction.

Data are presented in Figs. 5 and 6 by Weisz and Prater [8], where effects are evident as the diffusional resistance is increased with increasing particle size.

It is very important to account properly for this masking during the interpretation of laboratory or

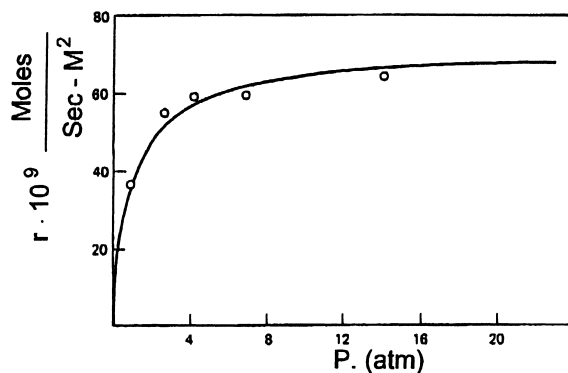


Fig. 5. The effect of diffusion transport on a zeroth order reaction. Pressure dependence in the cracking of cumene on silica alumina. After Weisz and Prater [8], by permission from Academic Press.

pilot plant kinetic data in order to avoid pitfalls in the scale-up procedure.

This can be performed using a simple criterion proposed in the same paper by Weisz and Prater [8]. They noted that the parameter

$$\Phi = \eta \cdot \phi^2 = \left(\frac{V_p}{S_p}\right)^2 \cdot \frac{r}{D_{es} \cdot C} \quad (14)$$

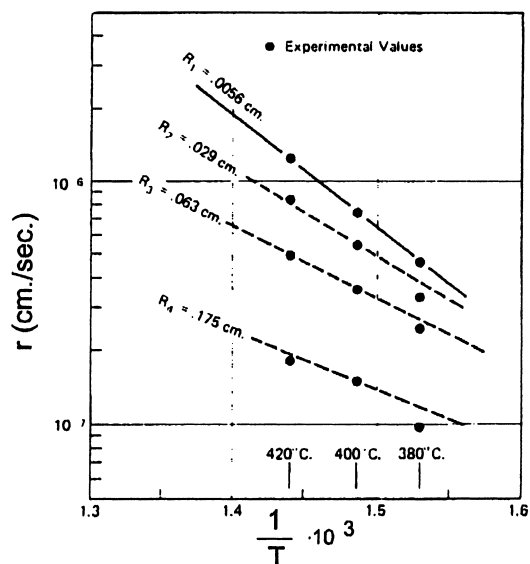


Fig. 6. Experimental demonstration of the effect of diffusion on the measured activation energy of the cracking of cumene on $\text{SiO}_2\text{--Al}_2\text{O}_3$ catalyst. After Weisz and Prater [8], by permission from Academic Press.

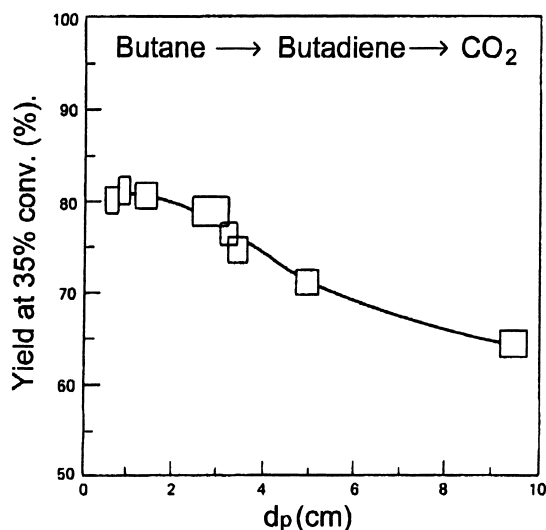


Fig. 7. Yield of butadiene at 35% conversion as a function of particle size using an iron oxide catalyst at 620°C. Reprinted with permission from Voge and Morgan [9]; © 1972 American Chemical Society.

is an observable quantity (combination of the experimental reaction rate r of the bulk concentration C and of other measurable quantities) and from their study they found that diffusion limitations are insignificant if $\Phi \leq 1$.

2.3.2. Diffusional disguise of selectivity of isothermal catalytic pellet

In [3,7] we can find the mathematical treatment of important general cases: parallel and consecutive reactions.

In Fig. 7 we can see the yield of a consecutive reaction as a function of particle size from the work of Voge and Morgan [9].

In Fig. 8 relative yield ratio versus Φ for the parallel reaction scheme studied by Roberts [10] are shown; the particular case presented considers the rate $A \rightarrow B$ by first order and $A \rightarrow C$ by second order kinetics.

The impact of reactions happening with volume change $A_1 \rightarrow mA_2$ on the effectiveness factor has been studied by Weekmann and Goring [11]; in Fig. 9 an example of their calculations with η'/η (relative effectiveness factor which accounts for volumetric change to that which neglects it) as a function of volume change modulus $\alpha' = (m-1)C/C_{\text{Tot}}$, at different values of Thiele modulus ϕ , is reported.

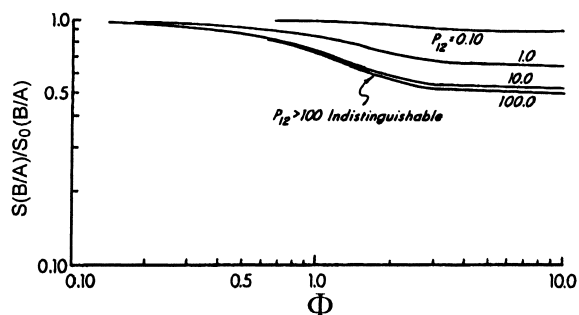


Fig. 8. Relative yield ratio vs. modulus Φ for various values of $P_{12} = k_1/(k_2C)$ first and second order reaction. Reprinted from Roberts [10]; © 1972 with permission from Pergamon Press.

2.4. The influence of thermal gradients

The solution of differential equations describing a single nonisothermal chemical reaction $A_1 \rightarrow \text{products}$ inside a catalytic pellet bring to the following inter- and intrapellet temperature gradients. Defining by $\text{Max}(T_s)$ the maximal intraparticle temperature (inside the pellet), we find after some mathematics following the work of Luss [3]:

$$\frac{\text{Max}(T_s) - T_{ss}}{T_{ss}} = \beta, \quad (16)$$

$$\frac{T_{ss} - T}{T} = \frac{\beta_G \cdot \Phi}{Bi_p}, \quad (17)$$

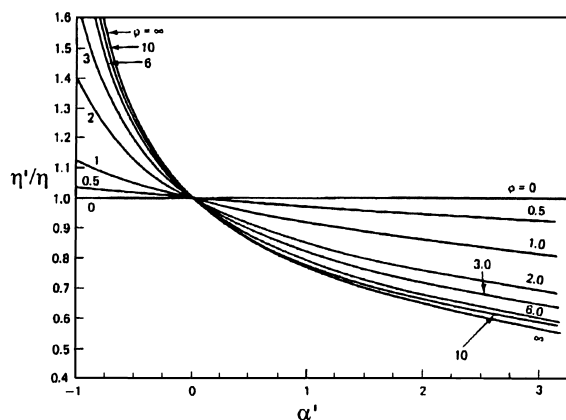


Fig. 9. Relative effectiveness factor η'/η vs. volume change modulus α' for a second order reaction in a spherical pellet. After Weekmann and Goring [11], by permission from Academic Press.

ratio internal/external temperature difference:

$$\frac{\text{Max}(T_s) - T_{ss}}{T_{ss} - T} = \frac{Bi_p}{Sh^*} \left(\frac{Sh^*}{\Phi} - 1 \right), \quad (18)$$

where Bi_p (Biot number) = $h_g \cdot V_p / \lambda_{es} \cdot S_p$, Sh^* (modified Sherwood number) = $\epsilon_s \cdot k \cdot V_p / D_{es} \cdot S_p$, β (Prater number) = $(-\Delta H) \cdot D_{es} \cdot C_{ss} / \lambda_{es} \cdot T_{ss}$, β_G (Prater number at bulk conditions) = $(-\Delta H) \cdot D_{es} \cdot C / \lambda_{es} \cdot T$.

Significant temperature gradients can exist only when the observed reaction rate is not too small. When the reaction is mass transfer limited, $\Phi \rightarrow Sh^*$ and Eq. (18) predicts that intraparticle temperature gradients are negligible. It follows that significant intraparticle temperature gradients exist only for intermediate values of Φ/Sh^* . For most operating conditions $Sh^* \gg Bi_p$. Consequently, interparticle thermal resistances usually are larger than intraparticle ones. This is opposite as in the diffusional resistance for which intraparticle gradients usually exceed the interparticle ones.

One of the key factors affecting the ratio between the two thermal gradients is the effective conductivity of the solid. This is shown quite clearly in Fig. 10, where Kehoe and Butt [12] measured the inter- and intraparticle temperatures during the hydrogenation of benzene on Ni catalysts using two supports with a 10-fold difference in conductivity and hence in Bi_p number.

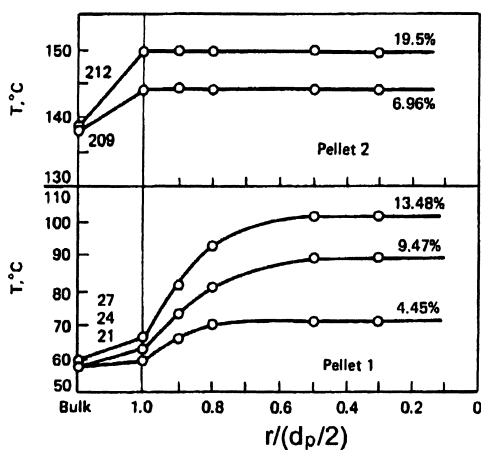


Fig. 10. Measured internal and external temperature profiles in the hydrogenation of benzene on Ni as a function of feed composition for two pellets of different conductivities. Reproduced with permission from the American Institute of Chemical Engineers, Kehoe and Butt [12]. © 1972 AIChE. All rights reserved.

2.5. Steady state multiplicity

A catalytic pellet may present multiple steady state solutions for the same set of parameters. This may happen in cases of:

Complex reaction network and/or particular kinetic expression. In several reactions one of the reactants may be adsorbed so strongly that a reduction of its concentration will increase the reaction rate; this behaviour may cause the existence of nonunique steady state solutions for some values of the Thiele modulus as pointed out by Roberts and Satterfield [13] where the case of bimolecular Langmuir–Hinshelwood kinetics is treated.

Heat production inside the pellet. Weisz and Hicks [14] examined the influence of intraparticle temperatures gradients for a first order irreversible reaction neglecting the external heat and mass transfer resistance, and computed the η - ϕ graph of Fig. 11: η exceeds unity for several values of the parameters.

This occurs when the increase in the reaction rate due to internal temperature gradients overcompensates the decrease in reaction rate due to mass transfer resistance.

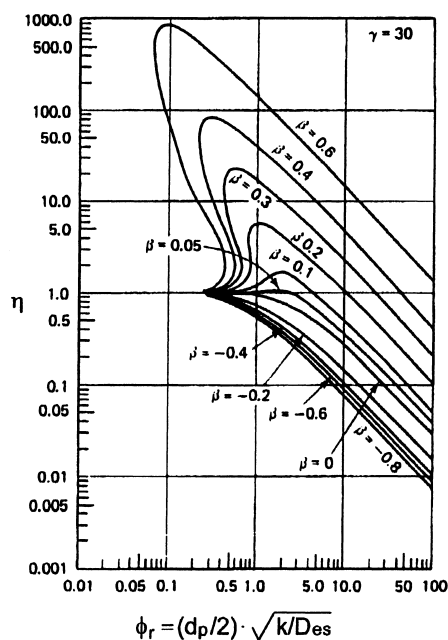


Fig. 11. Effectiveness factor vs. Thiele modulus for a first order irreversible reaction in a spherical catalytic pellet. β =Prater number. Reprinted from Weisz and Hicks [14]; © 1962 with permission from Pergamon Press.

sates for the reduction in the rate due to concentration gradients. Fig. 11 shows that in certain cases several values of η correspond to the same ϕ indicating that internal temperature gradients may cause steady state multiplicity. Several uniqueness criteria have been derived. For a first order reaction in a spherical pellet, Luss [3] pointed out that neglecting the external heat and mass transfer resistance:

$$\beta \cdot \gamma < 4 \cdot (1 + \beta), \quad (19)$$

where γ =[dimensionless activation energy]= E/RT provided a good estimate of condition for uniqueness.

A list of parameters $\beta \cdot \gamma$ and γ for reaction of industrial interest is given in Table 2.

Coupling of reaction kinetics with the characteristics of heat and mass transfer between pellet and surrounding fluid. Combining external and internal gradients also has an effect on the possible unstable behaviour of the catalytic pellet. There is more chance for multiplicity at reasonable values of the parameters. Criteria for these events to occur have been derived by several investigators; see [2,3] for the development of criteria.

The ability to predict a priori the kinetic parameters and operating conditions for which steady state multiplicity occurs presents practical relevancy in order to find a suitable working point for the pellet and hence for the reactor, out from situations of potential instability.

2.6. Design parameter and criteria

Considering a reacting system in a catalytic pellet we face a set of dimensionless parameters (β_i , γ_i , ϕ_j , Sh_j , Nu). For a given reaction network, with known

heats of reaction, intrinsic kinetic rates, and known properties of the pellet, the main design parameters are:

The dimension of shaped catalyst (d_p) which is the most important parameter; considering a situation with constant internal structure of the pellet, with the increase of catalyst dimension (when required by considerations at macroscopic scale), there can be a dramatic change of performances of the catalyst by decreasing conversion and yield.

The reagents concentration which affects the β_i , β_{Gi} and hence the thermal behaviour of the catalyst.

The pore volume ϵ_s and its distribution among micro-, meso- and macropores. When the reactor performance requires bigger catalyst dimensions, we can try to increase ϵ_s – when catalyst production techniques and mechanical properties allow us to – and/or to optimise the distribution among micro-, meso- and macropores.

The distribution of active components. When diffusional limitations cannot be avoided, in the presence of expensive active components, a common practice is to limit the quantity employed distributing the active component in the external part of pellet near to the surface, where it effectively works.

It is worth to remind the relevance of *mechanical properties*; industrial pellets must satisfy requirements of stability not only in reacting conditions, but also in all the other operations (delivering, filling up of reactors, etc.).

3. Adiabatic reactors

In adiabatic reactors the catalyst is present in the form of a uniform fixed bed that is surrounded by an outer insulating jacket. The basic and most applied scheme is illustrated in Fig. 12(a).

Adiabatic reactors are used when there is no adverse effect on selectivity or yield due to the adiabatic temperature development and this may happen when the heat of reaction is small, there is only one major reaction pattern or there is an excess of one of the reactants.

In addition to the phenomena at the scale of pellet described in the previous chapter, macroscopic phenomena at the scale of the reactor are operating: the convection in the direction of the flow and heat and

Table 2
Dimensionless parameters $\beta \cdot \gamma$ and γ for some exothermic reactions (after Hlavacek et al. [15])

Reaction	$\beta \cdot \gamma$	γ
Ethylene oxidation	1.76	13.4
Methanol oxidation	0.175	16.0
Oxidation of SO ₂	0.175	14.8
H ₂ oxidation	0.21–2.3	6.75–7.52
Higher alcohols from CO+H ₂	0.024	28.4
Ammonia synthesis	0.0018	29.4
Dissociation of N ₂ O	1.0–2.0	14–16

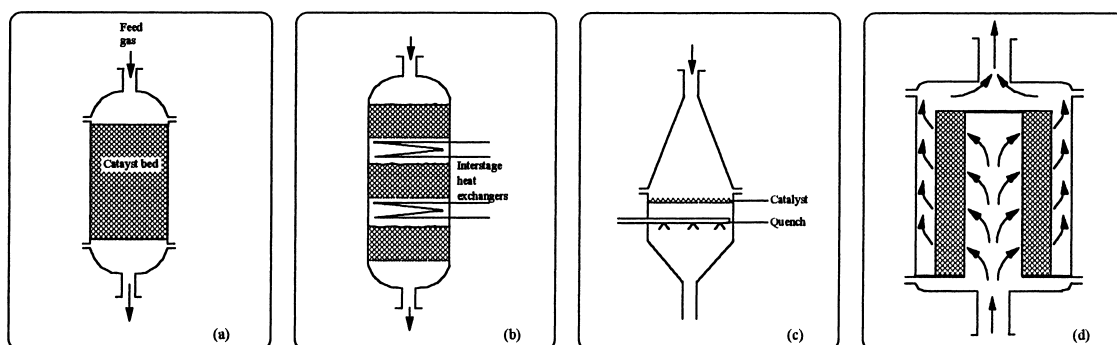


Fig. 12. Adiabatic reactors of different type.

mass dispersion effects which arise because of complex flow pattern and large spatial variations of concentration and temperature between the ends of the packed bed. For illustration purposes, Fig. 13 is presented.

3.1. The models

We refer to the general classification introduced by Froment [16] both for adiabatic and nonadiabatic reactors and reproduced in Table 3. For adiabatic

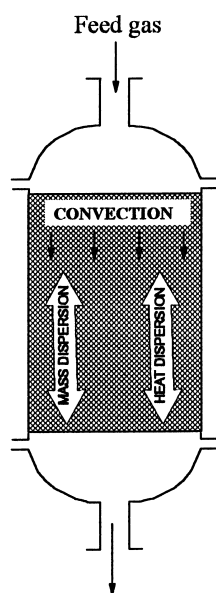


Fig. 13. Macroscopic transfer phenomena in axial reactor.

reactors, as mass and heat convection and dispersion effects are in the direction of flow, there is no need to consider bidimensional models.

If an exothermic reaction occurring in an adiabatic bed is associated with a mild heat generation, then pseudo-homogeneous models are suitable to describe the behaviour of the reactor.

As an example note ammonia synthesis, ethylbenzene dehydrogenation to styrene and methanol synthesis, etc.

The AI (plug-flow) model takes into consideration only the convective mechanism of heat and mass transfer and is frequently used to describe the behaviour of adiabatic packed bed for its simplicity. It is satisfactory for long packed beds and high linear velocity in the packing, reaction associated with low heat effects and small size of catalyst pellets.

For a reacting system of NS species and NR reactions, the mass balance for every component j and the heat balance are:

$$u \cdot \frac{dC_j}{dZ} - \rho_b \mathcal{R}_j(C, T) = 0, \quad (20)$$

$$u \cdot \rho_f \cdot c_{pf} \cdot \frac{dT}{dZ} - \rho_b \cdot \sum_i (-\Delta H_i) \cdot r_i(C, T) = 0 \quad (21)$$

with initial conditions: $Z=0$, $C_j=C_{0j}$, $T=T_0$.

The A II (dispersion) model takes into account the mixing in axial direction which is caused by turbulence and the presence of the packing: to the overall transport by plug-flow an effective mechanism of dispersion, described by dispersion coefficients, is superimposed. This model, apt for short beds (see

Table 3
Classification of fixed bed reactor models

A Pseudo-homogeneous ($T=T_s$, $C=C_s$)			B Heterogeneous ($T \neq T_s$, $C \neq C_s$)	
One-dimensional	A I	Basic, ideal, plug flow	B I	+Interfacial gradients
	A II	+Axial mixing	B II	+Intraparticle gradients
Two-dimensional	A III	+Radial mixing	B III	+Radial mixing

Fig. 12(c)), is given by the following equations:

$$\epsilon \cdot D_{\text{eaj}} \cdot \frac{d^2 C_j}{dZ^2} - u \cdot \frac{dC_j}{dZ} + \rho_b \cdot \Re_j(\underline{C}, T) = 0, \quad (22)$$

$$\lambda_{\text{ea}} \cdot \frac{d^2 T}{dZ^2} - u \cdot \rho_f \cdot c_{\text{pf}} \cdot \frac{dT}{dZ} + \rho_b \cdot \sum_i (-\Delta H_i) \cdot r_i(\underline{C}, T) = 0 \quad (23)$$

with b.c.: $Z=0$,

$$-\epsilon \cdot D_{\text{eaj}} \cdot \frac{dC_j}{dZ} = u \cdot (C_{0j} - C_j), \quad (24)$$

$$-\lambda_{\text{ea}} \cdot \frac{dT}{dZ} = u \cdot \rho_f \cdot c_{\text{pf}} \cdot (T_0 - T); \quad (25)$$

$Z=L$,

$$\frac{dC_j}{dZ} = \frac{dT}{dZ} = 0. \quad (26)$$

This model presents a nonlinear boundary value problem requiring an iterative approach in the integration.

If a strongly exothermic reaction occurs such as, e.g., oxidation of ethylene, carbon monoxide, or ammonia etc., then heterogeneous models, which take into account different conditions on the surface of the pellet and in the gaseous phase due to mass and heat transfer resistance, are needed.

The most general model (the B II one of Table 3—+heat and mass dispersion) was developed by Hlavacek and Votruba [17] in order to model ignition-extinction phenomena:

$$-\epsilon \cdot D_{\text{eaj}} \cdot \frac{d^2 C_j}{dZ^2} + u \cdot \frac{dC_j}{dZ} + k_g a (C_j - C_{\text{ssj}}) = 0, \quad (27)$$

$$-\lambda_{\text{ea}} \cdot \frac{d^2 T}{dZ^2} + u \cdot \rho_f \cdot c_{\text{pg}} \cdot \frac{dT}{dZ} + h_g a \cdot (T - T_{\text{ss}}) = 0, \quad (28)$$

with b.c.: $Z=0$,

$$-\epsilon \cdot D_{\text{eaj}} \cdot \frac{dC_j}{dZ} = u \cdot (C_{0j} - C_j), \quad (29)$$

$$-\lambda_{\text{ea}} \cdot \frac{dT}{dZ} = u \cdot \rho_f \cdot c_{\text{pf}} \cdot (T_0 - T); \quad (30)$$

$Z=L$,

$$\frac{dC_j}{dZ} = \frac{dT}{dZ} = 0. \quad (31)$$

These equations coupled with the ones at microscopic scale suitable to describe an isothermal pellet with diffusion limitations (Eqs. (2)–(6b)) constitutes the whole model. The computing problem is quite relevant and can be simplified using a precalculated effectiveness factor for the reaction rate expression.

Concerning the complexity of the model the best practice is to consider the simplest model with all the main relevant phenomena and then add complexity only when needed by comparison between experimental and calculated data.

3.2. Dimensionless parameters

Considering the heterogeneous dispersion model and a single reaction of n th order $A_1 \rightarrow \text{products}$, after introducing dimensionless variables $Z^* = Z/L$, $C^* = C/C_0$, $C_{\text{ss}}^* = C_{\text{ss}}/C_0$, $\Theta = E \cdot (T - T_0)/R \cdot T_0^2$ and $\Theta_{\text{ss}} = E \cdot (T_{\text{ss}} - T_0)/R \cdot T_0^2$, we face the following dimensionless parameters:

$$Bo_{aL} = \text{Bodenstein number} = \frac{u \cdot d_p}{\epsilon \cdot D_{\text{ea}}} \cdot \frac{L}{d_p} = Bo_a \cdot \frac{L}{d_p}, \quad (32)$$

$$Pe_{aL} = \text{Peclet number} = \frac{u \cdot \rho_f \cdot c_{\text{pf}} \cdot d_p}{\lambda_{\text{ea}}} \cdot \frac{L}{d_p} = Pe_a \cdot \frac{L}{d_p}, \quad (33)$$

$$\mathfrak{J}_D = \frac{k_g a \cdot L}{u}, \quad (34)$$

$$\mathfrak{I}_H = \frac{h_g a \cdot L}{\rho_f \cdot c_{pf} \cdot u}, \quad (35)$$

$$Da = \text{Damkohler number} = \frac{r(C_0, T_0) \cdot L}{C_0 \cdot u} \\ = \frac{A \cdot \exp(-E/RT_0) \cdot C_0^{n-1} \cdot L}{u}, \quad (36)$$

$$B = \text{dimensionless adiabatic temperature rise} \\ = \frac{(-\Delta H) \cdot C_0}{\rho_f \cdot c_{pf} \cdot T_0} \cdot \frac{E}{R \cdot T_0} = (\beta_G)_0 \cdot \gamma, \quad (37)$$

where Bo_a , Pe_a are based on pellet diameter and Bo_{aL} , Pe_{aL} are based on reactor length L .

To these the known parameters: β , γ , ϕ sum up. Remind that \mathfrak{I}_D and \mathfrak{I}_H , somehow related to Nu (h_g) and Sh (k_g), are already known from the previous chapter. $(\beta_G)_0$ is the Prater number evaluated at the bulk conditions and at the reactor inlet.

3.3. Current design data in adiabatic fixed bed reactors

For pressure drop calculation, the Ergun correlation is recommended:

$$\frac{\Delta P}{L} = \left(\frac{150 \cdot (1 - \epsilon) \cdot \mu}{d_p} + 1.75 \cdot G \right) \cdot \frac{(1 - \epsilon)}{\epsilon^3} \cdot \frac{G}{d_p \cdot \rho_f \cdot g_c}. \quad (38)$$

For ΔP calculation in reactors is preferable to express $\Delta P/L$ as $\text{grad } P$ (dP/dZ for a tubular reactor) and then compute the total pressure drop $\Delta P = \int_0^L (\text{grad } P) dZ$ along the flow direction Z considering the variation of ρ_f with T , P and the volume change due to reaction.

For axial mass dispersion coefficient, the correlation based on the work of Edwards and Richardson [18] and tested by Wen and Fan [19] on many experimental data valid for $0.08 \leq Re \leq 400$ and $0.28 \leq Sc \leq 2.2$ can be adopted:

$$\frac{1}{Bo_a} = \frac{D_{ea}}{v \cdot d_p} = \frac{0.5}{1 + 9.5 \cdot \epsilon / (Re \cdot Sc)} + \frac{0.75 \cdot \epsilon}{Re \cdot Sc}. \quad (39)$$

In Fig. 14 Eq. (39) is presented with $9.5 \cdot \epsilon \cong 3.8$ and $0.75 \cdot \epsilon \cong 0.3$, where the authors express Bo_a as Pe_a (Peclet number in axial direction). For Reynolds number high enough Bo_a is near or equal to 2; note that (at enough high Re) for the components of a multicomponent mixture all the Bo_{aj} becomes equal ($\cong 2$).

Axial heat dispersion coefficients can be evaluated from Dixon and Cresswell [20]:

$$\frac{1}{Pe_a} = \frac{\lambda_{ea}}{u \cdot \rho_f \cdot c_{pf} \cdot d_p} = \frac{\lambda_{af}}{u \cdot \rho_f \cdot c_{pf} \cdot d_p} + \frac{\lambda_{as}/\lambda_f}{Re \cdot Pr} + \frac{u \cdot \rho_f \cdot c_{pf}}{ah \cdot d_p}. \quad (40)$$

For Re high enough Pe_a is near or equal to 2.

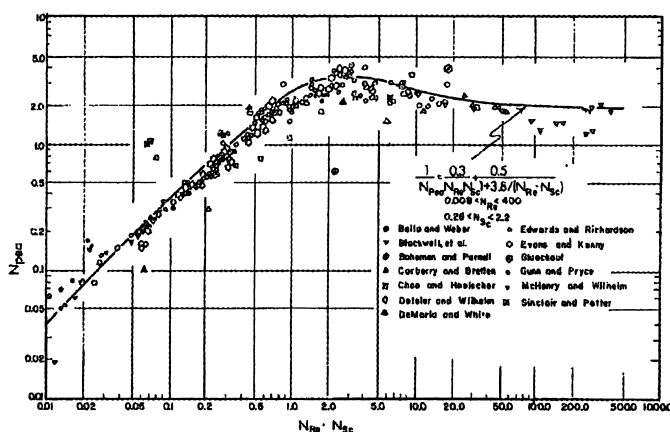


Fig. 14. Correlation of axial dispersion. Coefficient for gases flowing through fixed beds. Reprinted from Wen and Fan [19], p. 171 by courtesy of Marcel Dekker.

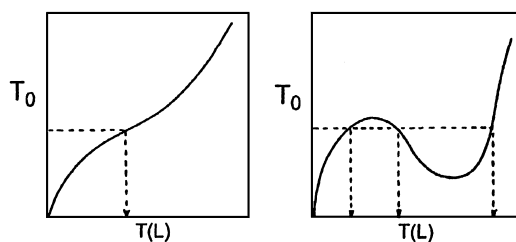


Fig. 15. One-dimensional tubular reactor with axial mixing. Outlet vs. inlet temperature.

3.4. Multiple steady states

The A II model (Eqs. (22)–(26)) has received great attention because the introduction of axial mixing leads to the possibility of more than one steady state profile through the reactor. In Fig. 15 the relationship between the inlet temperature T_0 and the outlet temperature $T(L)$ in two situations with increasing Da ($1/Bo_a$) is presented: in the second case three solutions are feasible. The presence of multiple steady state is more probable for a strongly exothermic reaction.

For a first order reaction the following condition presented by Hoffmann and Hlavacek [21] governs the occurrence of multiplicity:

$$B > \frac{4 \cdot \gamma}{\gamma - 4}. \quad (41)$$

If this condition is satisfied, then for a given value of Pe_{aL} number a region of Da number exists where multiple steady states occur. For higher values of Pe_{aL} this region contracts and over a critical Pe_{aL} number only unique states occur.

As already pointed out, it is very important to know a priori if more than one steady state is possible in order to determine the optimal design in a range of parameters where only single solutions are possible. Froment [16] analyses the situation in industrial processes and states that multiplicity will occur in region of parameters quite far from that of industrial practice. Hlavacek and Votruba [17] are not so categorical and show the experimental data obtained studying the oxidation of CO in a pilot reactor (see Fig. 16), data which did require the development of the model presented before in Eqs. (27)–(31) and Eqs. (2)–(5a) and (6b) to have reasonable agreement between the experimental and measured extinction point.

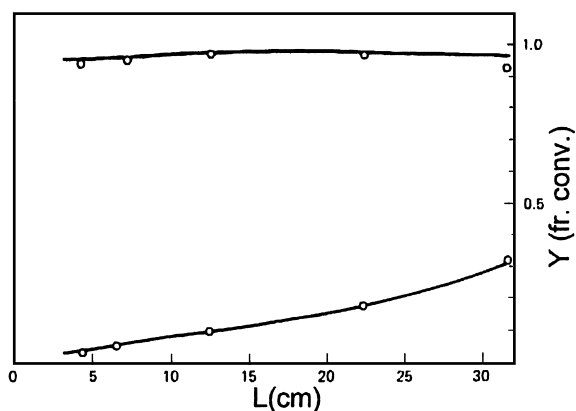


Fig. 16. Measured region of multiple solutions: carbon monoxide oxidation. After Hlavacek and Votruba [17], by permission from Prentice-Hall.

3.5. Design parameters and criteria

Considering a reacting system in a tubular adiabatic reactor, we face a certain number of parameters (in dimensionless terms to the already known β_i , γ_i , ϕ_j , Sh_j , Nu , the Bo_{aj} , Da_i , Pe_a should be added). For a given reaction system, with known heats of reaction, intrinsic kinetic rates and for a given catalyst with known internal characteristics the design parameters for a given production rate are:

- the dimension of shaped catalyst;
- the inlet reactants concentration C_{0j} ;
- the linear velocity (or the ratio d_t/d_p);
- the ratio L/d_p ;
- the inlet temperature.

The C_{0j} are usually not an independent variable because they influence the energy consumption required in the separation section so that the value of inlet concentrations comes from an optimisation between reaction section and separation section.

When possible, we should choose:

- inlet concentrations not too high in order to obtain reasonable adiabatic temperature rise (low B) which would avoid possible problems of multiple steady states;
- linear velocities high enough to avoid problems of interparticle heat (and mass) transfer and of axial dispersion (unless for very short beds);

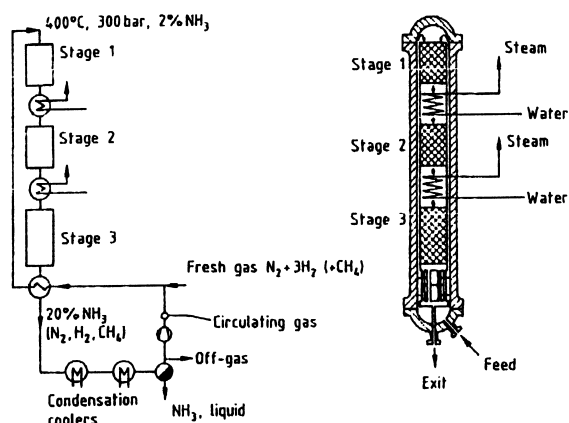


Fig. 17. Schematic picture of a multistage reactor for ammonia synthesis. Reprinted from [33]; by permission from Wiley–VCH.

- a reactor length L not too high in order to keep the pressure drop ΔP reasonably low.

When the adiabatic temperature rise B becomes too high we can adopt the multistage reactor layout with heat exchange between stages as in Fig. 12(b); this concept is very important for reactions limited by chemical equilibrium as in the example of Fig. 17 for the ammonia synthesis.

The tubular adiabatic reactor may present limitations in the scaling up: when very high production capacities are required the ΔP may become an insuperable limit.

In order to overcome these problems reactors with radial flow (Fig. 12(d)) have been developed. They make higher throughput and hence higher capacity possible, because of the low pressure drop and moreover, it is also possible to use smaller particles with higher effectiveness factor.

With reference to Fig. 12(d) and taking into account the following assumptions: channelling and shortcut effects do not occur; absence of gradients in axial and angular direction; all the models described previously can be considered (see [17] for examples about models and design parameters correlations). As examples of industrial application we find the dehydrogenation of ethylbenzene and the ammonia synthesis.

3.6. The autothermal reactors

Since the incoming reaction gases in most cases must be heated to the ignition temperature of the

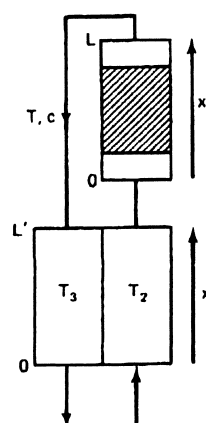


Fig. 18. Autothermal reactor.

catalytic reaction, adiabatic reaction control is often coupled with heat exchange between the incoming and exiting reaction gas producing the so-called autothermal reactor (Fig. 18).

Hlavacek and Votruba [17] present a thorough analysis of autothermal reactors devoted also to the study of multiple steady states. In the schematic description of Fig. 19, the heat generation curve and possible heat withdrawal lines are presented indicating the possible presence of multiple steady states. So attention has to be devoted in design of these reactors in order to avoid situations of instability.

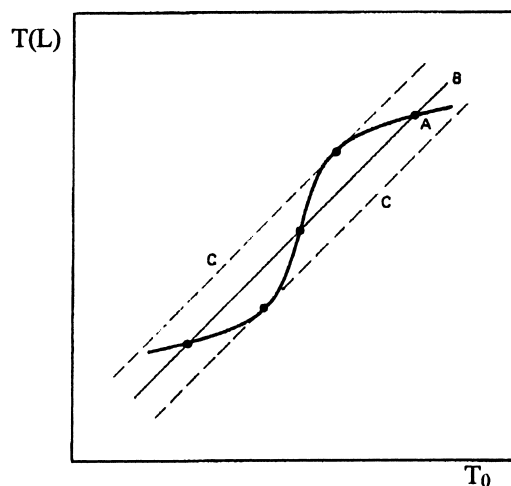


Fig. 19. Steady states in an autothermal reactor: (A) heat generations; (B) heat transfer; (C) limiting positions. After Hlavacek and Votruba [17]; by permission from Prentice-Hall.

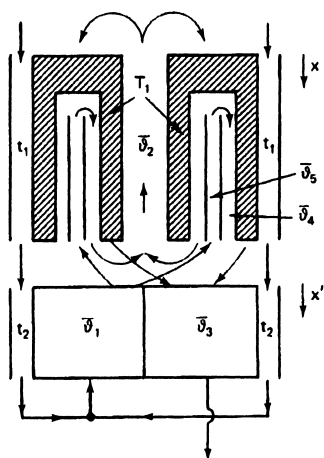


Fig. 20. The NEC ammonia synthesis. After Hlavacek and Votruba [17], by permission from Prentice-Hall.

As an example of industrial application of autothermal reactors we can consider the NEC ammonia synthesis reactor (Fig. 20).

An other important application is the autothermal reaction control with direct, regenerative heat exchange developed by Matros [22] in which the catalyst packing simultaneously acts as the regenerative heat exchanger. Fig. 21 shows the basic arrangement. After the catalytic fixed bed has been heated to the reaction temperature, for example with a burner, the cold reaction gas flows into the packing, where it is

heated by the hot catalyst packing and then reacts. At the same time the inflow part of the packing is cooled so that the reaction front migrates into the packing. Before the reaction front has reached the end of the packing, the flow direction is reversed by valves so that the temperature front moves back again and heats the cooled part of the packing. In this way a periodic steady state is finally established. The upper and lower ends of the bed serve as regenerative heat exchanger, the hot central as reaction zone.

3.7. Dynamics and control

Fixed bed reactors of industrial relevance are generally operated in a stationary mode. The target is usually there to keep the desired conversion constant. Mass flow control, feed stoichiometry control, control of the total pressure as well as feed temperature control are therefore the most important automatic control circuits in fixed bed reactors.

However, the nonstationary dynamic operation mode is also of great importance for industrial operation control. Very interesting from this point of view is the experimental and modelling work done by Van Doesburg and De Jong [23] using the methanation of CO and CO₂ as test reaction carried out in a 0.5 l adiabatic catalytic reactor in mild conditions. The axial temperature profile was measured as a function of time after applying changes in feed concentration

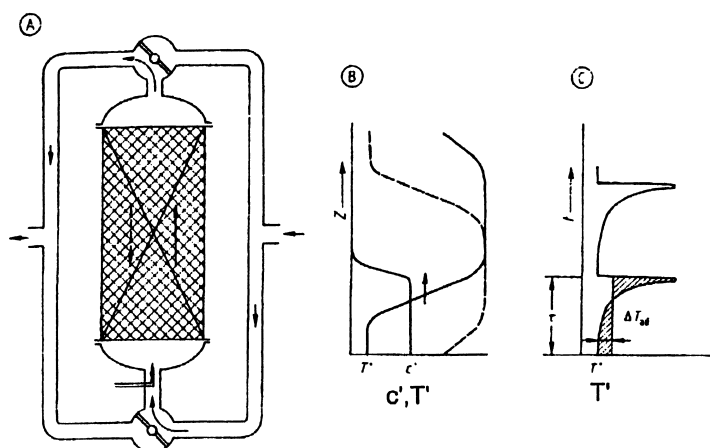


Fig. 21. Autothermal reaction control with direct (regenerative) heat exchange for an irreversible reaction: (A) basic arrangement; (B) local concentration and temperature profiles prior to flow reversal in steady state; (C) variation of outlet temperature with time in steady state. After Eigenberger and Nicken [22]; by permission from Wiley-VCH.

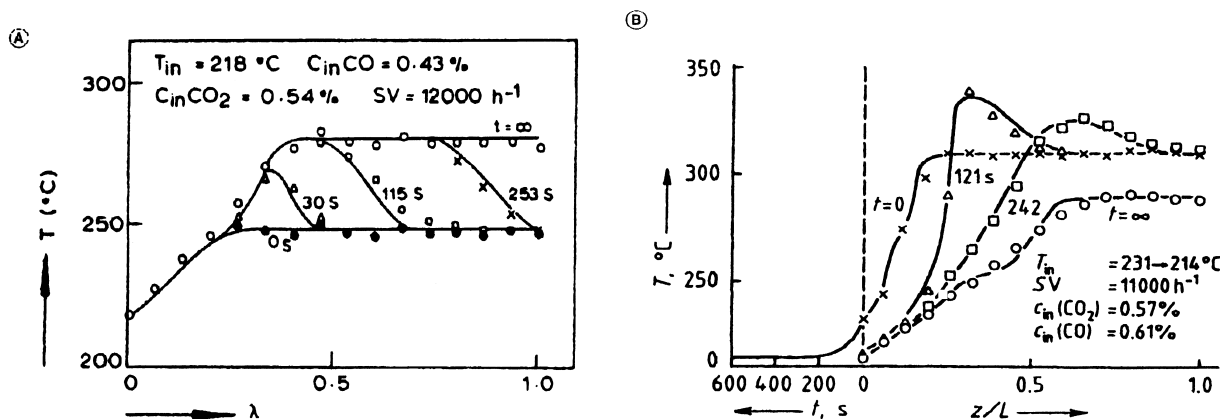


Fig. 22. Measured (points) and calculated temperature profiles showing the transient of an adiabatic fixed-bed reactor for the methanation of CO and CO₂: (A) transition after increasing the feed concentration; (B) transition after decreasing the feed temperature. SV=space velocity. Reprinted from Van Doesburg and De Jong [24]; © 1976 with permission from Pergamon Press.

(increase and decrease) and decreases in the inlet temperature. In Fig. 22(a) and (b), the experimental data and calculated temperature profiles obtained with a quasi-homogeneous model solved using the Crank–Nicholson algorithm are reported.

When the feed concentration is increased a new main reaction zone forms in the front part of the reactor and the temperature rises gradually to a new maximum value. When the feed temperature is decreased, the maximum temperature in the fixed bed initially increases rapidly (the “wrong way behaviour”) and then the main reaction zone moves slowly in direction of the outlet reaching at the end a new stationary state at lower temperature.

3.8. Monolith structures

Monolithic catalysts are continuous unitary structures which contain many small, mostly parallel passages. A ceramic or metallic support is coated with a layer of material in which active ingredients are dispersed. They are particularly suited when pressure losses must be kept low, as in cases where the reaction conversion is low and a large circulating gas ratio has been considered as well for the off-gas purification, in which large off-gas streams must be handled with minimal additional cost. The common operating condition is the adiabatic one. In Table 4 and Fig. 23 typical geometries are presented.

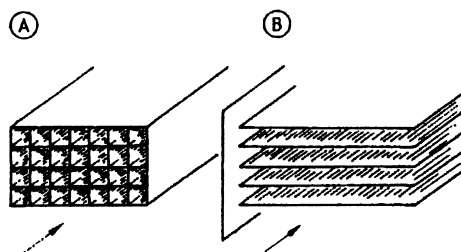


Fig. 23. Usual shapes of monolith catalysts: (A) square-channel monolith; (B) parallel-plate monolith.

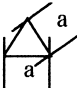
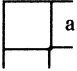


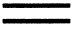
Monolithic structures are presently used to solve important industrial problems such as control of automotive emissions, abatement of waste exhaust gases, nitrogen oxide emission control.

There are advantages of monolithic structures over the classical packed bed concept:

- the monolithic support has much higher geometric surface area;
- the honeycomb matrix has a very low pressure drop because of the existence of straight channels in the monolithic structure.

The honeycomb support should have moreover characteristics to suit the process: attrition-resistance to the operating conditions caused by gas flow and/or vibrations experienced during vehicle operations, and also resistance to deposition of carbon and dust.

Table 4
Asymptotic dimensionless laminar flow heat or mass transfer coefficients $Nu=\alpha_w \cdot d_h/\lambda_g$ (constant wall conditions) and Fanning friction factor f for pressure drop $\Delta p = 2f(\eta Z_L/d_h^2) \cdot v_g$ for ducts of different cross section (after Shah [24])

Geometry	Nu	f	d_h
	2.47	13.33	$2a/\sqrt{3}$
	2.98	14.23	a
	3.34	15.05	$2\sqrt{3}a$
	3.66	16.00	a
	7.54	24.00	$2a$

Basic to the design of monolithic reactors is of course the knowledge of kinetics of the monolithic structure expressed per unit area of active surface and the heat and mass transfer effects.

In [17] we find geometric data, correlations for Peclet, Nusselt and Sherwood and for pressure drop and models which are able to describe the reactor performance.

Industrial applications range from largest reactor used to remove NO_x from power station flue gases (DeNO_x process), with a catalyst volume more than 1000 m³ with several monolithic units as shown in Fig. 24, to the smallest reactor for the catalytic treatment of the exhaust gases of internal combustion engines with one monolithic unit of about 1 l (Fig. 25).

4. Nonisothermal nonadiabatic tubular reactors

Nonadiabatic reactors are used when the adiabatic temperature development is high and influences the selectivity of the reaction; in these reactors indirect heat exchange occurs via a circulating heat transfer medium integrated in the fixed bed. They can also be adopted because a better isothermal behaviour can produce better performances as for example in the dehydrogenation of ethylbenzene to styrene to compensate the unfavourable reaction rate at lower temperatures.

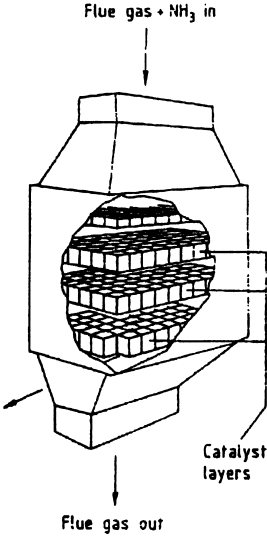


Fig. 24. Reactor chamber for removal of nitrogen oxides from power station flue gas. After Steinmueller [33].

The most common arrangement is the multitubular fixed bed reactor in which the catalyst is arranged in tubes and the heat carrier circulates externally around the tubes (see Fig. 26(a)–(c)).

Owing to the poor heat transfer characteristics of the system what should be an “isothermal fixed bed reactor” has really a quite different behaviour with significant temperature profiles in the axial and radial

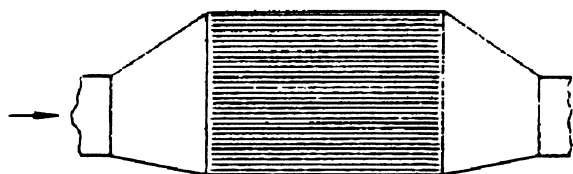


Fig. 25. Catalytic after burner for internal combustion engines. After Eigenberger and Nicken [22], by permission from Wiley–VCH.

direction as illustrated in Fig. 27. The peak type axial temperature profile is the so-called “hot spot”.

4.1. The models

The mathematical models suitable for the description of these complex phenomena are the already known models used for the adiabatic reactors to which the transport of heat and mass in the radial direction is superimposed, as pointed out in the aforementioned Table 3.

The simplest model is the A I (plug flow):

$$u \cdot \frac{dC_j}{dZ} - \rho_b \cdot \Re_j(\underline{C}, T) = 0, \quad (42)$$

$$u \cdot \rho_f \cdot c_{pf} \cdot \frac{dT}{dZ} - \rho_b \cdot \sum_i (-\Delta H_i) \cdot r_i(\underline{C}, T) + \frac{4 \cdot U}{d_t} \cdot (T - T_w) = 0 \quad (43)$$

with initial conditions $Z=0$:

$$C_j = C_{0j}, \quad T = T_0, \quad (44)$$

where U is the overall heat transfer coefficient with the cooling medium.

But owing to the pronounced heat effect in radial direction, it is natural to prefer and rely on models able to predict the detailed temperature and conversion patterns in the reactor and this leads to two-dimensional models, where the flux of heat or mass in the radial direction is modelled by the effective transport concept. In the majority of industrially important cases axial dispersion of mass and heat can be omitted following the considerations already done with the adiabatic reactors.

The continuity equations for the j component and the energy equation for pseudo-homogeneous two-dimensional model with a reaction system of NS compounds and NR reactions are:

$$- \epsilon \cdot D_{erj} \cdot \left(\frac{\partial^2 C_j}{\partial R^2} + \frac{1}{R} \cdot \frac{\partial C_j}{\partial R} \right) + u \cdot \frac{\partial C_j}{\partial Z} - \rho_b \cdot \Re_j(\underline{C}, T) = 0, \quad (45)$$

$$- \lambda_{er} \cdot \left(\frac{\partial^2 T}{\partial R^2} + \frac{1}{R} \cdot \frac{\partial T}{\partial R} \right) + u \cdot \rho_f \cdot \frac{\partial T}{\partial Z} - \rho_b \cdot \sum_i (-\Delta H_i) \cdot r_i(\underline{C}, T) = 0 \quad (46)$$

with b.c.:

$$Z = 0, 0 \leq R \leq (d_t/2), \quad C_j = C_{0j}, \quad T = T_0, \quad (47)$$

$$0 \leq Z \leq L, R = 0,$$

$$\frac{\partial C_j}{\partial R} = 0, \quad \frac{\partial T}{\partial R} = 0, \quad (48)$$

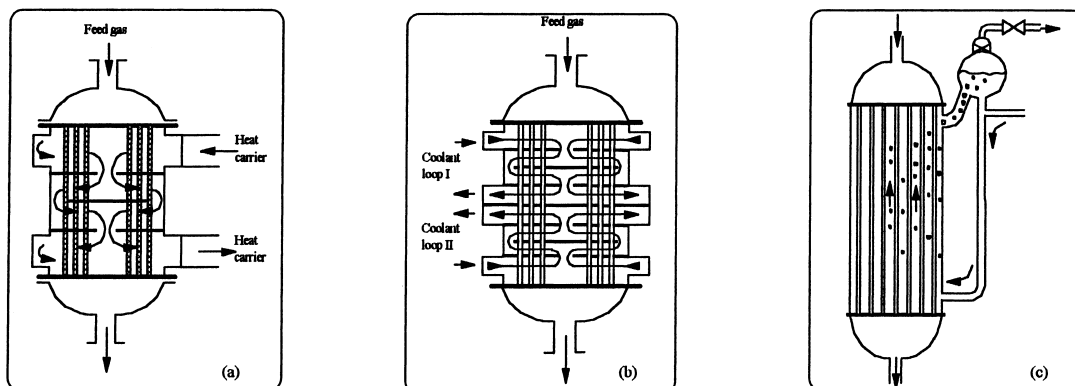


Fig. 26. Nonisothermal–nonadiabatic tubular reactors.

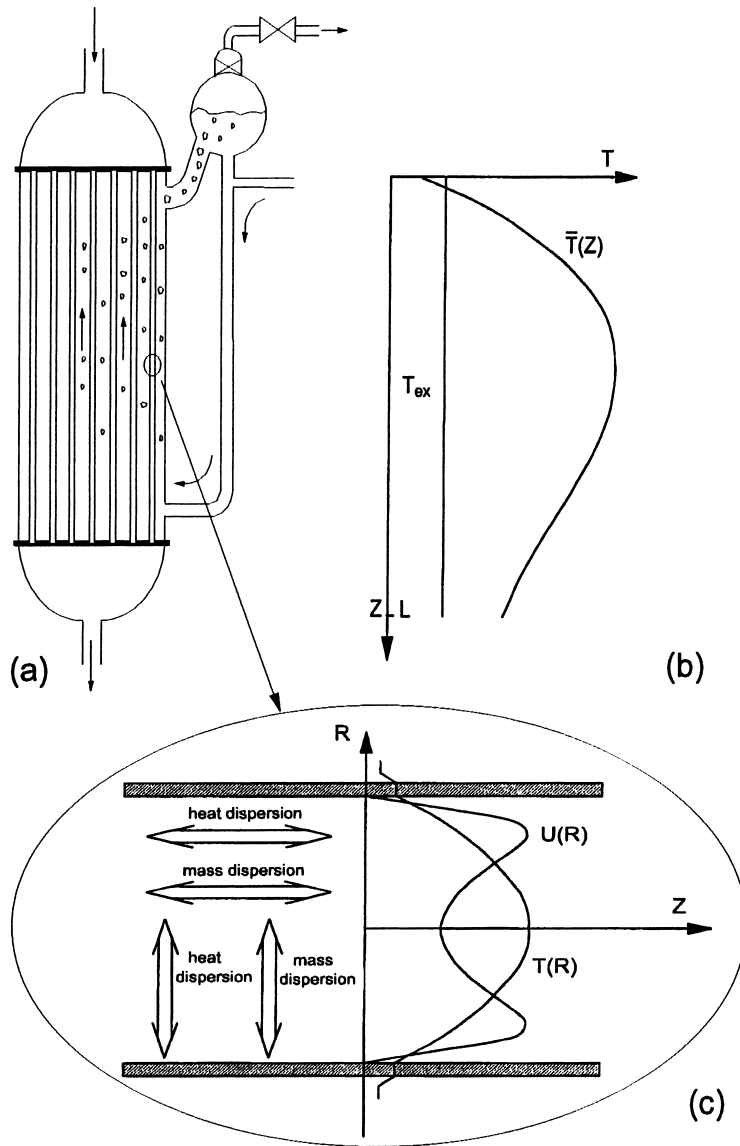


Fig. 27. Tubular reactor: (a) basic scheme; (b) axial profile of mean radial temperature; (c) basic scheme of axial and radial dispersion phenomena and radial profiles of temperature and velocity.

$$R=(d_t/2),$$

$$\frac{\partial C_j}{\partial R} = 0, \quad \frac{\partial T}{\partial R} = -\frac{\alpha_w}{\lambda_{er}} \cdot (T - T_w), \quad (49)$$

The effective thermal conductivity λ_{er} , constant in the core of tubular reactor, becomes higher near the wall; the usual approach considers a mean value of λ_{er} and a second coefficient accounting for the heat transfer at the wall α_w defined by Eq. (49).

With strong exothermic reactions gas to solid heat and mass transfer play an important role and in this case the choice is for the heterogeneous two-dimensional model:

$$\begin{aligned} -\epsilon \cdot D_{erj} \left(\frac{\partial^2 C_j}{\partial R^2} + \frac{1}{R} \cdot \frac{\partial C_j}{\partial R} \right) + u \cdot \frac{\partial C_j}{\partial Z} \\ + k_{gj} a \cdot (C_j - C_{ssj}) = 0, \end{aligned} \quad (50)$$

$$-\lambda_{er} \cdot \left(\frac{\partial^2 T}{\partial R^2} + \frac{1}{R} \cdot \frac{\partial T}{\partial R} \right) + u \cdot \rho_f \cdot c_{pf} \cdot \frac{\partial T}{\partial Z} + h_g a \cdot (T - T_{ss}) = 0 \quad (51)$$

with b.c.:

$$Z = 0, C_j = 0, T = T_0,$$

$$0 \leq Z \leq L,$$

$$R = 0,$$

$$\frac{\partial C_j}{\partial R} = 0, \quad \frac{\partial T}{\partial R} = 0, \quad (52)$$

$$R = (d_p/2),$$

$$\frac{\partial C_j}{\partial R} = 0, \quad \alpha_w \cdot (T_w - T) = \lambda_{er} \cdot \frac{\partial T}{\partial R}. \quad (53)$$

Eqs. (50)–(53) coupled with the ones at pellet scale Eqs. (2)–(6b) constitutes the whole model. The computing problem can be simplified using an effectiveness factor.

4.2. Dimensionless parameters

With reference to a single reaction, by transforming the previous equations in dimensionless ones, after introducing the dimensionless variables $Z^* = Z/L$, $R^* = R/(d_p/2)$, $C^* = C/C_0$, $C_s^* = C_s/C_0$, $\Theta = E \cdot (T - T_0)/R \cdot T_0^2$ and $\Theta_s = E \cdot (T_s - T_0)/R \cdot T_0^2$, we take into consideration the following new dimensionless parameters which sum up to the already known β , γ , ϕ , Sh , Nu , Bo_a , Pe_a , Da , B :

$$Bo_r = \text{Bodenstein number in radial direction} = \frac{v \cdot d_p}{D_{er}}, \quad (54)$$

Pe_r = Peclet number in radial direction

$$= \frac{u \cdot \rho_f \cdot c_{pf} \cdot d_p}{\lambda_{er}}, \quad (55)$$

$$Bi_i = \text{Biot number} = \frac{\alpha_w \cdot d_p}{\lambda_{er}}. \quad (56)$$

4.3. Design data

Effective radial conductivity and apparent wall heat transfer coefficient are proposed by Dixon [25]:

$$\lambda_{er} \cdot \frac{Bi}{Bi + 4} = \lambda_{rf} \cdot \frac{Bi_f}{Bi_f + 4} + \lambda_{rs} \cdot \frac{Bi_s}{Bi_s + 4}, \quad (57)$$

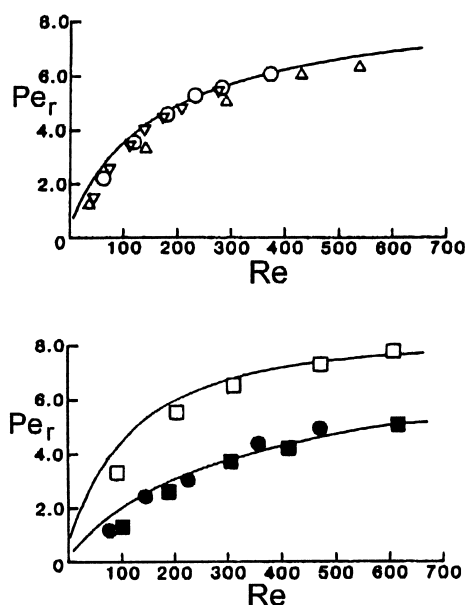


Fig. 28. Radial Peclet number vs. Reynolds number: (a) same thermal conductivity; (b) different thermal conductivity (nylon vs. steel). Reproduced with permission of the American Institute of Chemical Engineers, Dixon [25]. © 1985 AIChE. All rights reserved.

where

$$Bi_i = \frac{\alpha_w \cdot (d_p/2)}{\lambda_{er}} = \begin{cases} Bi_{if} (= \alpha_w \cdot (d_p/2)/\lambda_{rf}) & (\text{high } Re; Re > 1000), \\ Bi_{is} (= \alpha_w \cdot (d_p/2)/\lambda_{rs}) & (\text{low } Re; Re < 10). \end{cases}$$

In Figs. 28 and 29 Pe_r and Bi are reported as a function of Re .

For the radial mass dispersion, De Ligny [26] adopted the following correlation:

$$\frac{1}{Bo_r} = \frac{\tau_b}{Re \cdot Sc} + \frac{a}{1 + (b/Re \cdot Sc)}. \quad (58)$$

For spherical packing τ_b the tortuosity factor is 0.67 and $a=0.12$, $b=78 \pm 20$.

For practical purposes Pe_r and Bo_r may be considered to lie between 8 and 10.

4.4. Examples of application

The reliability of the models can be tested only by comparison with experimental data.

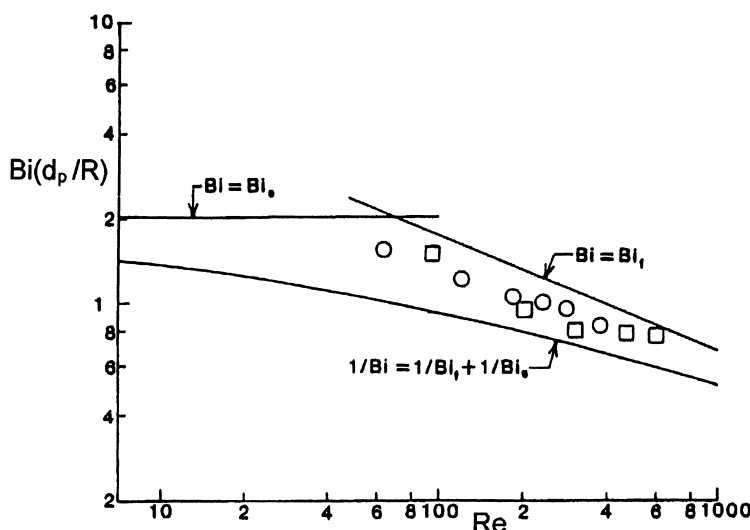


Fig. 29. Comparison of formulas for Bi with data for 9.5 mm ceramic spheres and nylon spheres ($d_i/d_p=7.6$). Reproduced with permission of the American Institute of Chemical Engineers, Dixon [25]. © 1985 AIChE. All rights reserved.

The work done some years ago in EniChem [27] with the vinylacetate synthesis from acetylene and acetic acid with Zn acetate supported on carbon can help. With reference to Fig. 30, the work was concerned with:

- kinetic measurements on catalytic pellets using a Bertly type reactor and determination of the kinetic model of Langmuir–Hinselwood kind with reference to the main reaction (in the range of conversion 0–60% the selectivity is very high); kinetic results were not influenced by the size of pellets indicating an effectiveness factor very near to one.
- heat transfer measurements in the pilot reactor/heat exchanger described in Fig. 30(a); in order to simplify the regression of the data, the inlet temperature profile was carefully made constant along the radius $T(Z,0)=T(Z,d_i/2)$. The measured parameters are shown in Fig. 30(b) and (c).
- measurements of conversion in the same reactor/heat exchanger of Fig. 30(a). Inlet temperature was kept constant along the radius and temperature profiles were measured in the presence of reaction. The interpretation of the experimental results was performed using the two-dimensional pseudo-homogeneous model and the experimentally measured parameters – without the need of any “tuning” – just adding to the model the

correlation of Fahien and Stankovic [28] in order to take into account the velocity profile along the radius, which presents a maximum at $1.5d_p$ from the reactor wall.

The results shown in Fig. 30(d)–(f) indicate the accuracy of the model. The application of these studies to the industrial scale brought to a better design of the reactor with a smaller diameter.

4.5. Parametric sensitivity and run away

Nonisothermal–nonadiabatic reactors do not present real problems of instability but rather of *parametric sensitivity*, which is the exaggerated response of the behaviour of the reactor, e.g. in terms of thermal profile and conversion in correspondence with small variations of operating parameters. This happens when the heat transfer capacity of the system is not fully adequate with respect to the production rate of the heat generated by the reaction. In this situation the reactor control is a difficult task and imperceptible changes of operating conditions may produce the complete loss of control of the reactor: the run away.

A priori criteria can be found for single reaction. Dente and Collina [29] approaching the sensitivity problem with a A I model state that reactor’s behaviour present:

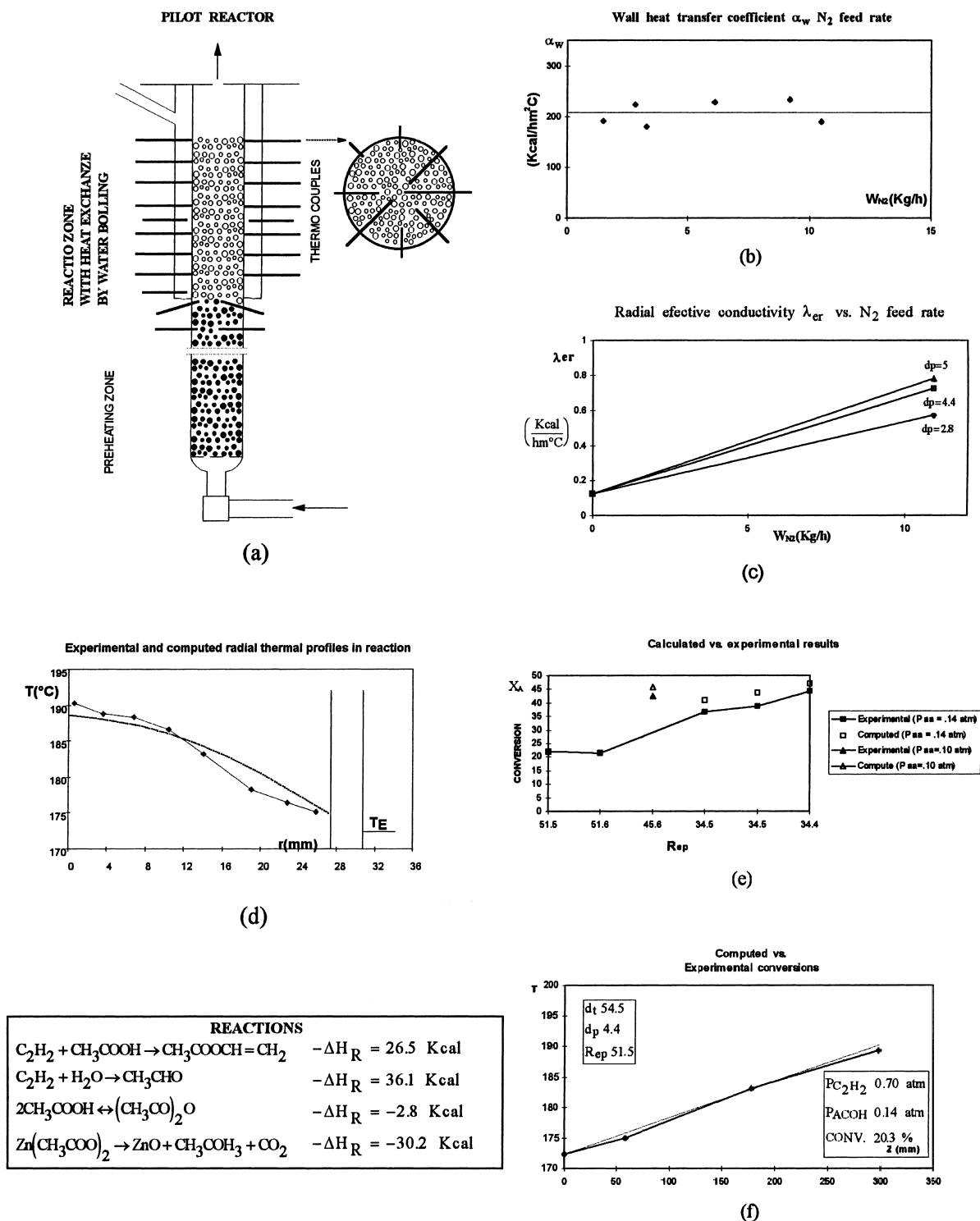


Fig. 30. Study of vinyl acetate reactor.

1. no sensitivity with a temperature profile satisfying the conditions: $d^2\Theta/dDa^2 < 0$ at any point before the maximum temperature, i.e. with $d\Theta/dDa^2 > 0$ (Θ and Da defined in Section 3.2);
2. sensitivity when the temperature profile has $d^2\Theta/dDa^2 > 0$ in some interval before the maximum.

Van Velsenaere and Froment [30] inspecting by an A I model the temperature and partial pressure profiles of an oxidation reaction conclude that parametric sensitivity and run away may be possible:

1. when the hot spot exceeds a certain value;
2. when the temperature profile obtained with a simple plug-flow model develops inflection points before its maximum (see Fig. 31).

For more complex situations we have to rely on the availability of models by which we can perform a parametric study; of course a suitable package of data are needed: kinetic data, heat and mass transfer correlations for the reactor and for the catalytic particle, etc.

4.6. One- vs. two-dimensional models

The models described in Eqs. (45)–(49) and Eqs. (50)–(53) are a set of partial parabolic differen-

tial equations, which are rather difficult to solve even with the today's computing facilities. A simplification is often made which approximates the partial differential equations by a set of ordinary differential equations: resulting model assumes that concentration and temperature gradients occur only in the axial direction, dealing therefore with average values of concentration and temperature in radial direction.

Finlayson [31] approached the problem with a orthogonal collocation procedure, where the collocation point, representative of the mean concentrations and temperature in radial direction, is chosen by a suitable polynomial; using e.g. the Legendre polynomial the collocation point is at $R^* = \sqrt{2}/2$ and the overall heat transfer coefficient U is given by

$$\frac{1}{U} = \frac{1}{\alpha_w} + \frac{d_t}{8 \cdot \lambda_{cr}}. \quad (59)$$

The two dimensional models will become mono-dimensional with the possibility of maintaining some information on the radial behaviour. For example, the radial temperature profile is given by [17]:

$$T^*(R^*) = T_c^* + \frac{1 - R^{*2} + 2/Bi}{1 - R_1^{*2} + 2/Bi} \cdot (T^*(R_1^*) - T_c^*), \quad (60)$$

where R_1^* is $\sqrt{2}/2$ and T_c^* is the dimensionless temperature of the cooling medium.

In this way we can describe the reactor with simpler equations useful in preliminary studies and for control problems.

4.7. Design parameters

Considering a reacting system in a tubular reactor, we face a certain number of parameters and dimensionless terms β_i , γ_i , ϕ_j , Sh_j , Nu , Bo_{aj} , Bo_{rj} , Da_i , Pe_a , Pe_r . For a given reaction system with known heats of reaction, intrinsic kinetic rates and for a given catalyst with known internal characteristics, the design parameters for a given production rate (with reference to a single tube) are:

- the pellet diameter;
- the ratio d_i/d_p ranging from 8 to 50;
- the ratio L/d_p ;
- the inlet concentration and temperature;
- the temperature of cooling medium.

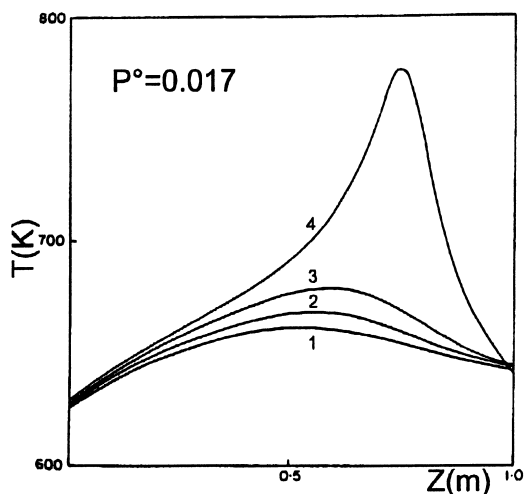


Fig. 31. Temperature profiles in reactor showing the sensitivity with respect to inlet temperature. (1) $T_0=T_w=625$ K, (2) $T_0=T_w=627$ K, (3) $T_0=T_w=626$ K, (4) $T_0=T_w=628$ K. Reprinted from Van Velsenaere and Froment [30], © 1970 with permission from Pergamon Press.

The adoption of design values is heavily conditioned by the constraints of avoiding the situations of parametric sensitivity and runaway. Very critical is the ratio d_r/d_p which conditions the heat transfer from the pellets in the core of the reactor to the wall. If necessary in order to limit the hot spot temperature also extreme values of about 4–5 can be chosen.

In order to compensate the ageing of the catalyst very often much higher quantities of catalyst are used and therefore attention has to be paid to ΔP value which should be kept at a reasonable limit for energy consumption reasons (usually $\Delta P \leq 0.5$ – 1 kg/cm²).

4.8. Control of fixed bed reactors

The control of fixed bed reactors is strictly related to the design of the reactor: a good design will choose the optimum operating conditions far from the region of parametric sensitivity and hence from runaway conditions.

The target is usually there to keep the desired conversion constant. Mass flow control, feed stoichiometry control, control of the total pressure as well as feed temperature and heat transfer medium temperature control are therefore the most important automatic control circuits in fixed bed reactors.

5. Conclusions

The theory of fixed bed reactors enables us to:

- interpret the experimental data in laboratory (kinetics and diffusion), pilot and reactor scale and simulate the behaviour of reactors using models which range from the very simple to the very complicated and therefore are able to suit to the complexity of the system and to the availability of the data required;
- understand the characteristics and the limits of the system under study: presence of mass and/or heat transfer resistances inside or outside the pellet, the relevance or not of dispersion phenomena;
- design a reactor choosing the best operating conditions outside the region of multiple steady states or of parametric sensitivity which is the region of potential instabilities in order to guarantee a good control of the reactor.

6. Symbols

a	specific area of pellet/packing (m ² /m ³)
A	pre-exponential factor (s ⁻¹) (for first order reaction)
A_j	chemical compound j
B_i (Bi_p)	Biot number = $\alpha_w \cdot d_p / \lambda_{er}$ ($= h_g \cdot d_p / \lambda_{es}$)
Bo_a (Bo_r)	Bodenstein number = $v \cdot d_p / D_{ea}$ ($= v \cdot d_p / D_{er}$)
C (C_j)	concentration (of j) in the bulk gas (kmol/m ³)
c_{pf}	specific heat coefficient of fluid (gas) (kcal/kg °C)
C_s (C_{sj})	concentration (of j) inside the catalytic pellet (kmol/m ³)
C_{ss} (C_{ssj})	concentration (of j) at pellet surface (kmol/m ³)
D_{ea} (D_{er})	dispersion coefficient in axial (radial) direction (m ² /s)
D_{es} (D_{esj})	effective diffusion coefficient of j inside the catalyst (m ² /s)
D_{ij}	binary diffusion coefficient of compounds i and j (m ² /s)
D_{jm}	diffusion coefficient of j in a multi-component system (m ² /s)
d_h	hydraulic diameter (m)
D_{Kj}	Knudsen diffusion coefficient of compound j (m ² /s)
d_p	pellet diameter (m)
d_t	reactor diameter (m)
E (E')	activation energy (apparent activation energy) (kcal/kmol)
$\mathfrak{Z}_D, \mathfrak{Z}_H$	dimensionless parameters defined by Eqs. (34) and (35)
G	specific mass flow = $u \cdot \rho_f$ (kg/m ² s)
g_c	dimensional constant (kg m/(kg _{force} s ²))
h_g	heat transfer coefficient (kcal/m ² s °C)
j_D, j_H	j -factor for mass, heat transfer
k	kinetic constant (s ⁻¹) (first order)
k'	kinetic constant (s ⁻¹ m ³ /kg) (first order)
k_g (k_{gj})	mass transfer coefficient (of j) (m/s)
L	reactor length (m)
M_j	molecular weight of j (kg/kmol)
n (n')	reaction order (apparent reaction order)
Nu	Nusselt number = $h_g \cdot d_p / \lambda_f$
ΔP	pressure drop of reactor (kg _{force} /cm ² or kPa)

Pe_a (Pe_r)	Peclet number= $u \cdot \rho_f \cdot c_{pf} \cdot d_p / \lambda_{ea}$ (= $u \cdot \rho_f \cdot c_{pf} \cdot d_p / \lambda_{er}$)
Pr	Prandtl number= $c_{pf} \mu_f / \lambda_f$
r	radial coordinate of pellet ($0 \leq r \leq d_p/2$) (m)
r	reaction rate (kmol/kg cat s)
R	radial coordinate of reactor (m)
$\geq R_j$	rate of production of compound $j = \sum_{i=1}^{NR} \nu_{ij} \cdot r_i$ (kmol/kg cat s)
Re	Reynolds number= $u \cdot d_p \cdot \rho_f / \mu_f$
S_p	external surface of the pellet (m^2)
Sc_j (Sc_j)	Schmidt number $Sc_j = \mu_f / \rho_f D_{jm}$
Sh (Sh_j)	Sherwood number $k_{gj} \cdot d_p / D_{jm}$
T	temperature in the reactor (K)
T_s	temperature inside the catalytic pellet (K)
T_{ss}	temperature on the surface of the catalytic pellet (K)
u	fluid velocity referred to whole section of reactor (m/s)
U	overall heat transfer coefficient (kcal/ $m^2 s ^\circ C$)
v	interstitial fluid velocity= u/ϵ (m/s)
V_p	pellet volume (m^3)
y	molar fraction
Z	axial coordinate (m)

Greek letters

α_w	wall heat transfer coefficient (kcal/ $m^2 s ^\circ C$)
β, β_G	Prater number with respect to surface, bulk conditions
ϵ (ϵ_s)	bed voidage fraction (internal porosity of catalyst)
ϕ_r (ϕ)	Thiele modulus for spherical pellet (generalised Thiele modulus)
Φ	defined by Eq. (13)
γ	dimensionless energy of activation
η, η_G	effectiveness factor with reference to C_s, C
λ_{as} (λ_{af})	axial thermal conductivity of solid (fluid) (kcal/kg $m ^\circ C$)
λ_f	thermal conductivity of the fluid (kcal/ kg $m ^\circ C$)
λ_{es}	effective thermal conductivity of the pellet (kcal/kg $m ^\circ C$)
$\lambda_{ea}, \lambda_{er}$	effective axial, radial thermal conduc- tivity of reactor (kcal/kg $m ^\circ C$)

$\lambda_{rs}, \lambda_{rf}$	radial thermal conductivity of solid, fluid (kcal/kg $m ^\circ C$)
μ_f	viscosity of fluid (gas) (Pa s)
ν_{ij}	stoichiometric coefficient of j in reac- tion i
ρ_f	density of fluid (gas) (kg/ m^3)
ρ_s	density of catalytic pellet (kg/ m^3)
ρ_b	density of catalytic bed (bulk density) (kg/ m^3)
Θ (Θ_{ss})	$E \cdot (T - T_0) / R \cdot T_0^2$ (= $E \cdot (T_{ss} - T_0) / R \cdot T_0^2$)
τ	tortuosity factor (τ_s of pellet, τ_b of reactor bed)

Subscript

a	axial
b	bulk conditions (concerning the gas phase but also the catalytic bed)
c	concerning the cooling medium
e	effective
f, g	concerning the fluid, gas
i	reaction i
j	compound j
0	at reactor inlet
r	radial, radius of spherical pellet and also pore radius
s	of the catalytic pellet
ss	at the pellet surface

Superscript

*	dimensionless variable, also modified dimensionless parameter
---	--

References

- [1] M.F.L. Johnson, W.E. Stewart, J. Catal. 4 (1965) 248.
- [2] R. Aris, The Mathematical Theory of Diffusion and Reaction in Permeable Catalysts, Clarendon Press, Oxford, 1975.
- [3] D. Luss, Steady-State and Dynamic Behaviour of a Single Catalytic Pellet, Chem. React. Theory – A Review, Prentice-Hall, Englewood Cliffs, NJ, 1977, pp. 191–268.
- [4] L.V.C. Rees, Studies in Surface Science and Catalysis, vol. 84, Elsevier Science, 1994, p. 1133.
- [5] J. Villadsen, M.L. Michelsen, Solution of Differential Equation Models by Polynomial Approximation, Prentice-Hall, Englewood Cliffs, NJ, 1978.
- [6] R.H. Perry, D.W. Green, Engineers Handbook, 6th ed., McGraw-Hill, New York, 1984.
- [7] G.F. Froment, K.B. Bischoff, Chemical Reactor Analysis and Design, 2nd ed., Wiley, New York, 1990, pp. 125–197.

- [8] P.B. Weisz, C.D. Prater, *Adv. Catal.* 6 (1954) 144.
- [9] H.H. Voge, C.Z. Morgan, *Ind. Eng. Chem. Process Des. Dev.* 11 (1972) 454.
- [10] G.W. Roberts, *Chem. Eng. Sci.* 27 (1972) 1409.
- [11] V.W. Weekmann, R.L. Gorrington, *J. Catal.* 4 (1965) 260.
- [12] J.P.G. Kehoe, J.B. Butt, *AIChE J.* 18 (1972) 595.
- [13] G.W. Roberts, C.N. Satterfield, *Ind. Eng. Chem. Fund.* 5 (1966) 317.
- [14] P.B. Weisz, J.S. Hicks, *Chem. Eng. Sci.* 17 (1962) 265.
- [15] V. Hlavacek, M. Kubicek, M. Marek, *J. Catal.* 15 (1969) 17.
- [16] G.F. Froment, *Analysis and Design of Fixed Bed Catalytic Reactors*, *Advances in Chemistry Series*, vol. 109, Am. Chem. Soc.-Washington, 1972, p. 1.
- [17] V. Hlavacek, J. Votruba, *Steady state operation of fixed bed reactors and monolithic structures*, *Chem. React. Theory – A Review*, Prentice-Hall, Englewood Cliffs, 1977, pp. 314–404.
- [18] M.F. Edwards, J.F. Richardson, *Chem. Eng. Sci.* 23 (1968) 109.
- [19] C.Y. Wen, L.T. Fan, *Models for Flow Systems and Chemical Reactors*, Marcel Dekker, New York, 1975, pp. 169–171.
- [20] A.G. Dixon, D.L. Cresswell, *AIChE J.* 32(4) (1986) 809.
- [21] H. Hoffmann, V. Hlavacek, *Chem. Eng. Sci.* 25 (1970) 173.
- [22] G. Eigenberger, U. Nicken, *Chem. Ing. Tech.* 63 (1991) 781.
- [23] H. Van Doesburg, W.A. De Jong, *Chem. Eng. Sci.* 31 (1976) (I) and (II) 45 (I) and 53 (II).
- [24] R.K. Shah, A.L. London, *Laminar Flow Forced Connection in Ducts*, *Advances in Heat Transfer*, Academic Press, New York, 1978.
- [25] A.G. Dixon, *AIChE J.* 31(5) (1985) 826.
- [26] C.L. De Ligny, *Chem. Eng. Sci.* 25 (1970) 1177.
- [27] D. Albertazzi, P. Andrigo, A. Caimi, *Vinyl acetate synthesis: study of reactor performance*, Enichem Internal Report, 1982.
- [28] R.W. Fahien, I.M. Stankovic, *Chem. Eng. Sci.* 34 (1979) 793.
- [29] M. Dente, A. Collina, *Chimica e Industria* 46 (1964) 1445.
- [30] R.J. Van Velsenaere, G.F. Froment, *Chem. Eng. Sci.* 25 (1970) 1503.
- [31] B.A. Finlayson, *Chem. Eng. Sci.* 26 (1971) 1081.
- [32] R. Aris, S. Rester, *Chem. Eng. Sci.* 24 (1969) 793.
- [33] G. Eigenberger, *Ullmann Encyclopedia of Industrial Chemistry*, *Fixed Bed Reactors*, vol. B4, 1992, p. 215.